Geomechanics and Engineering, *Vol. 16, No. 6 (2018) 599-608*
DOI: https://doi.org/10.12989/gae.2018.16.6.599

A simplified method to estimate the total cohesion of unsaturated soil using an UC test

Horn-Da Lin[1a], Chien-Chih Wang[*2] and Xu-Hui Wang[1b]

[1]*Department of Civil and Construction Engineering, National Taiwan University of Science and Technology, Taipei 10607, Taiwan*
[2]*Department of Civil Engineering and Geomatics, Cheng Shiu University, Kaohsiung 83347, Taiwan*

(Received November 16, 2017, Revised April 27, 2018, Accepted November 10, 2018)

Abstract. This study investigates the feasibility of adopting the results of the UC (unconfined compression) test to assess the total cohesion of the unsaturated soil. A series of laboratory tests were conducted on samples of unsaturated lateritic soils of northern Taiwan. Specifically, the unconfined compression test was combined with the pressure plate test to obtain the unconfined compression strength and its matric suction of the samples. Soil samples were first compacted at designated water content and then subjected to the wetting process for saturation and the subsequent drying process to its target suction using the apparatus developed by the authors. The correlations among the matric suction, the unconfined compression strength and the total cohesion were studied. As a result, a simplified method to estimate the total cohesion using the unconfined compressive strength is suggested. The calculated results compare reasonably with the unsaturated triaxial test results. Current results show good performance; however, further study is warranted.

Keywords: unsaturated soil; matric suction; total cohesion; unconfined compressive strength

1. Introduction

Cho (2016) comprehensively summarized that the future role of geotechnical engineering is essential for future sustainable development. One of the example problems is landslides due to typhoons and heavy rainfall occurring at an alarming rate in recent years due to El Niño and global warming. In Taiwan due to the continuous urbanization, infrastructure development and construction activities have extended from plains to laterite terraces such as the Linkuo terrace between Taipei city and Taoyuan international airport.

As the terrace is relatively high, the lateritic soil stratum is often above the groundwater table, thus, it is in the unsaturated state for the long-term. As water and air coexist in unsaturated soil pores, the capillary effect induces matric suction via the air-water interface (Fredlund and Morgenstern 1977, Fredlund *et al.* 1978). This suction may vary with the water content change due to rainfall infiltration and influence the behavior of unsaturated soils (Rahardjo *et al.* 2009, Oh and Vanapalli 2011, Ng *et al.* 2016, Kim *et al.* 2017, Tang *et al.* 2017). Therefore, for the analysis of slope stability of lateritic soils, matric suction should be considered in the evaluation of engineering properties (Lin *et al.* 2010). Soil parameters include the effective cohesion c', the effective friction angle ϕ', and the angle ϕ^b due to the effect of matric suction on the shear strength.

According to the extended Mohr-Coulomb failure criterion (Fredlund and Rahardjo, 1993), the total cohesion is the key strength parameter that can reflect the influence of matric suction. In essence, the total cohesion simultaneously takes into account of the effective cohesion and the contribution due to the matric suction. However, it may not be easy to determine the total cohesion because one must conduct rather complicated unsaturated triaxial tests to obtain this strength parameter. The authors have conducted some preliminary studies to develop simplified methods to assess the total cohesion (Lin *et al.* 2016, Lin *et al.* 2017). The results are encouraging but need further verification. Hence, this study investigates the feasibility of adopting test results of the UC (unconfined compression) strength, which is a common test in engineering practice, to assess the total cohesion of unsaturated lateritic soil. This simplified method is potential applicable to geotechnical engineering problems that require the knowledge of the unsaturated soil strength such as the landslide problem of unsaturated soil slope induced by rainfall infiltration (Lin *et al.* 2010, Zhang *et al.* 2014, Shou *et al.* 2018).

2. Test program

The soil samples were taken from the lateritic slope along National Highway No. 1 in Linkou area of northern Taiwan. A series of laboratory tests were conducted on samples of the compacted lateritic soil. The degree of saturation of the compacted soil is approximately 75% to 90% (Wang *et al.*, 2010, Yang *et al.* 2012). Unconfined

∗Corresponding author, Professor
E-mail: ccw@gcloud.csu.edu.tw
[a]Professor
E-mail: hdlin@mail.ntust.edu.tw
[b]M.Sc. Student
E-mail: w22639@gmail.com

ISSN: 2005-307X (Print), 2092-6219 (Online)

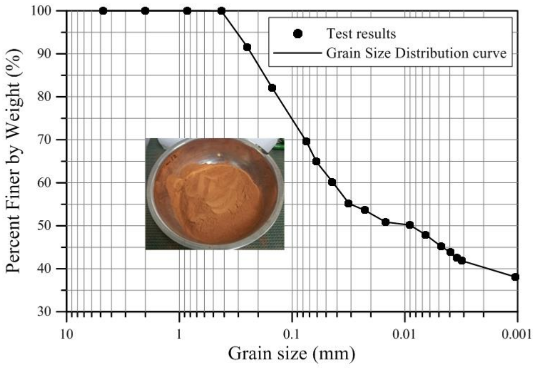

Fig. 1 Grain size distribution curve of Linkuo lateritic soil

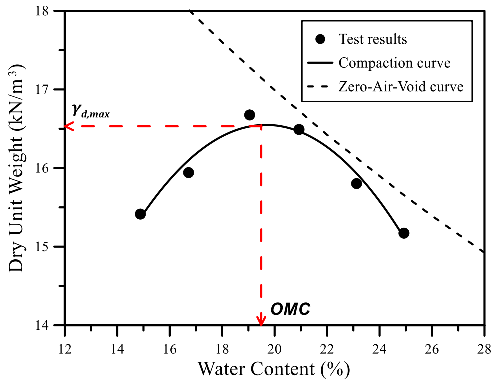

Fig. 2 Compaction curve of Linkuo lateritic soil

compression test was combined with pressure plate test to obtain the unconfined compression strength and matric suction of the samples. Soil samples were first compacted at the desired initial water content and then subjected to the designated wetting and drying using the apparatus developed by the authors. As a result, the correlations among the matric suction, the unconfined compression strength and the total cohesion can be studied under the framework of the extended Mohr-Coulomb model. For verification, unsaturated triaxial tests were also conducted. In addition, in order to effectively control the uniformity of the initial condition of the specimen, this study uses static compaction to remold the specimen, a machine to control the compaction energy, and molds to control specimen size, thus, reducing tester errors. Basic soil properties, sample preparation, and test procedures are elaborated below.

2.1 Soil property and specimen preparation

In this study, the specific gravity and the Atterberg limits are tested in accordance with ASTM D854-83 and ASTM D4318-10, respectively. The specific gravity of the soil Gs is 2.64, the liquid limit LL is 49, the plastic limit PL is 26, and the plastic index is 23. The grain size distribution test is performed in accordance to ASTM D452-85, as shown in Fig. 1. It is classified by USCS as CL (clay of low to medium plasticity) because the point of LL=49 and PI=23 plots just above the A-line of the plasticity chart. The x-ray diffraction tests show that main soil minerals are illite and quartz. For sample preparation, the modified compaction test were conducted according to ASTM D1557-12 (soil is compacted in five layers, each layer is tamped 25 times). Compaction test results show that the optimum moisture content (OMC) is 19.5% and the corresponding maximum dry soil unit weight is 16.6 kN/m^3, as shown in Fig. 2. In order to include the dry side and the wet side, three different initial compaction states (OMC-3%, OMC, OMC+3%) are selected for the specimen preparation. The corresponding dry unit weights are 16.0 kN/m^3, 16.6 kN/m^3, and 16.0 kN/m^3, respectively. The soil weight and water content of the remolded specimen are proportioned according to the modified compaction result. The well-mixed soil sample is put into a zipper bag for 24 hours to assure homogenization of water content. Afterwards, the soil is placed in the mold and compacted in five layers by static pressure into a remolded specimen with a diameter of 5 cm and height of 10 cm.

Fig. 3 Pressure plate test apparatus

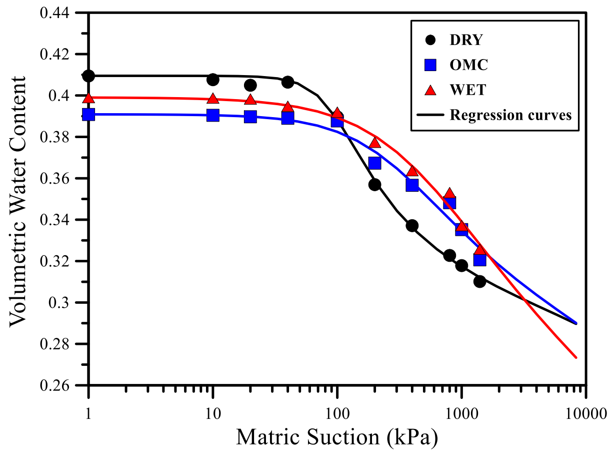

Fig. 4 SWCCs for different compaction conditions

2.2 Matric suction measurement

In this study, the pressure plate test was adopted for obtaining the Soil-Water Characteristic Curve (SWCC). Pressure plate extractors of 5 bar and 15 bar from Soilmoisture Equipment Corp. were used, as shown in Fig. 3. The pressure plate test is specified in ASTM D3152-72 including test procedures for measuring matric suction. The SWCC results were used to control the matric suction of the specimen for the unsaturated unconfined compression test.

More detailed procedures are to be discussed in the next section.

Three sets of soil samples were prepared at different initial water contents, including OMC-3% (DRY), OMC, and OMC+3% (WET). The test sets of OMC-3%, and OMC+3% are denoted as DRY and WET for easy reference. Samples were saturated and then put into the extractor for the pressure plate test. Samples were inundated with de-aired water and saturated in the oedometer following ASTM D2345-80. In general, samples can be saturated in about 2-3 days with a contact stress of 2.5 kPa. Ten stages of matric suction are applied to the soil sample, including 1, 10, 20, 40, 100, 200, 400, 800, 1000 and 1400 kPa. Test results are shown in Fig. 4. The SWCCs were regressed using the function suggested by Fredlund and Xing (1994). The SWCC results of three initial compaction conditions fall within the range of the SWCC results of four soil types ranging from sand to clay reported by Vanapalli *et al.* (1999). In addition, the air entry values and the shape of the SWCCs of the lateritic soil are similar to the results of the silt reported in that report.

Test results in Fig. 4 clearly show that volumetric water content decreases as suction increases, regardless of the initial compaction condition. In general, the trends of the SWCCs are similar. Notice that the initial volumetric water contents are somewhat different. The OMC is the densest and exhibits the smallest initial water content as expected. The dry density of the OMC-3% and OMC+3% is the same. However, the dry side sample exhibits larger initial water content than the wet side. This result is reasonable because the dry side sample adsorbed more upon saturation process due to its flocculated soil structure and larger swelling. To verify this observation water content change were measured before and after saturation of the sample. They are 7.6%, 5.0%, and 2.4% for the dry side, the OMC, and the wet side, respectively. Fig. 4 also show valuable information about the air entry value. The air entry value of the dry side is 62 kPa, which is the lowest. The air entry value of the wet side is 93 kPa, which is slightly less than that of the OMC (105 kPa). This tendency can be explained by the difference in soil structure. In general, the wet side sample exhibits dispersed structure and thus better water retention ability and larger air entry value.

2.3 Unsaturated unconfined compression test

The procedure for the unsaturated unconfined compression test can be summarized as follows: (1) prepare three sets of soil specimens at different initial compaction conditions of OMC-3%, OMC, and OMC+3%; (2) determine the desired water content of each specimen according to the target matric suction and the SWCCs in Fig. 4; (3) cure soil specimens to the desired water content using the wetting and drying apparatus; (4) conduct the unconfined compression test.

The matric suction of 100, 150, 200, 250, and 300 kPa were used. The matric suction of 100 kPa was selected based on the air entry values obtained from the SWCCs. Because when the suction exceeds the air entry value, the water content decreases significantly and the unsaturated soil behavior become more pronounced. The SWCCs in

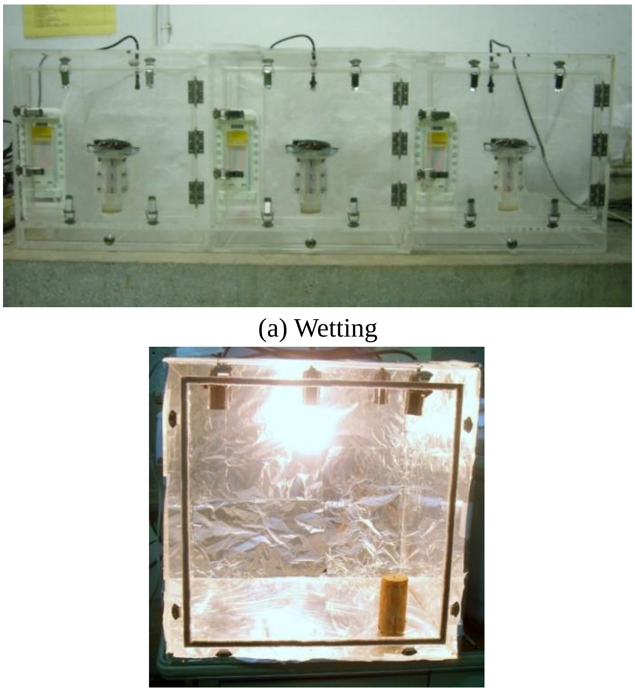

(a) Wetting

(b) Drying

Fig. 5 The wetting and drying apparatus

Fig. 4 were used to determine the desired water content of the unconfined compression test sample corresponding to the target matric suction. To achieve this task soil samples were prepared following the same procedure as that for the pressure plate test. To ensure the above procedure can get the desired matric suction some checks were conducted by measuring the matric suction using the filter paper method (ASTM D 5298-94). The results are satisfactory (Yang *et al.* 2008, Yang *et al.* 2012, Lin *et al.* 2016).

The wetting and drying apparatus is shown in Fig. 5. This environmental simulation system was developed by the authors and has been successfully used to repeatedly cure soil samples to the desired water content with good uniformity (Wang *et al.* 2010, Lin *et al.* 2015, Lin *et al.* 2016). The difference in moisture content between the measured values among different portions of the sample and the mean value is less than 0.5%. The wetting process is mainly achieved by the timer controlled sprinklers that are installed at the top of each wetting chamber. A light bulb is installed beneath the ceiling of the drying box to simulate sunshine drying. The temperature in the box was controlled approximately at 37°C to facilitate uniform evaporation of the soil specimen.

After the soil specimen has been prepared and cured to the target matric suction, the unconfined compression test (UC test) is conducted according to the test procedure specified by ASTM D2166-13. The strain rate suggested in this test standard is between 0.5%-2%/min. Fredlund and Rarardjo (1993) have suggested the strain rate of 0.102%/min for the undrained and unconfined test on unsaturated soil. Therefore, the strain rate of 0.102%/min was adopted in this study to ensure that the excess pore water pressure can be excited uniformly during the shearing process.

(a) Unsaturated triaxial cell

(b) Pressure control panel

Fig. 6 Photos of unsaturated triaxial apparatus

2.4 Unsaturated triaxial test

This study uses a self-developed facility for unsaturated triaxial testing. The test system consisted of the loading machine, the unsaturated triaxial cell, the pressure control panel, and the data acquisition devices, as shown in Fig. 6. The loading frame is made by ELE International of UK. Measuring devises are procured from well-known laboratory equipment companies such as Kyowa of Japan, Transcell of USA, etc. The unsaturated triaxial cell, the control panel and the data acquisition device were developed at National Taiwan University of Science and Technology (NTUST). This unsaturated triaxial system has been carefully calibrated and successfully used to conduct unsaturated triaxial tests (Yang *et al.* 2008, Jiang 2014, Lin *et al.* 2017).

In this study, the constant water content test (the CW triaxial test) was adopted. The CW test is one of the unsaturated triaxial tests suggested by Fredlund and Rarardjo (1993). In essence, the soil sample is compacted at the desired initial condition, saturated, and subjected to the target matric suction until it reaches equilibrium. Then, deviatoric loading is applied with the air pressure valve open and the back water pressure valve turned off. The excess pore water pressure is continuously measured during the deviator loading. Multistage triaxial test procedures proposed by Ho and Fredlund (1982) and Nyunt *et al.* (2011) are adopted in this study. When the deviator stress becomes almost constant, the soil sample was unloaded immediately and subjected to higher matric suction before reloading. The loading/unloading is repeated to obtain the shear strength parameters of the unsaturated soil under different predetermined suctions. In specific, the net normal pressure $(\sigma_n - u_a)$ is 50 kPa, and matric suctions are 100 kPa, 200 kPa, and 300 kPa, respectively. In addition, the strain rate of 0.102%/min which was the strain rate for the unconfined compression test was also selected for the unsaturated triaxial test.

2.5 Consolidated undrained test

The triaxial consolidated undrained (CU) test apparatus at NTUST was used to determine the effective cohesion and the effective friction angle. The CU test procedure follows ASTM D4767-11. Much effort has been made to assure the test results are accurate and repeatable. Three sets of samples were prepared at different initial compaction conditions (OMC-3%, OMC, and OMC+3%), following the same procedure described in the previous section. Each sample was saturated with backpressure and consolidated to the target effective confining pressure. The saturation process is consistent with the saturation process of the SWCC tests. The void ratio is not controlled during the saturation. In this study three effective confining pressures are adopted, including 50, 100, and 200 kPa. Subsequently, the deviator loading was applied to the consolidated sample until failure or 15% axial strain. The test results were then used to determine the effective cohesion and the effective friction angle.

3. Total cohesion of unsaturated soil

3.1 Total cohesion of the extended Mohr-Coulomb failure criterion

Fredlund *et al.* (1978) considered the contribution of matric suction to the shear strength of the unsaturated soil, and proposed the extended Mohr-Coulomb Criterion, which expands the two-dimensional Mohr-Coulomb failure envelope for saturated soils to the three-dimensional failure surface. The shear stress (τ) is used as vertical coordinates, while the net normal stress $(\sigma_n - u_a)$ and matric suction $(u_a - u_w)$ are horizontal coordinates. In the proposed criterion, the effect of matric suction can be explicitly quantified. The equation for the shear strength of the unsaturated soil is as follows

$$\tau_f = c' + (\sigma_n - u_a)_f \tan\phi' + (u_a - u_w)_f \tan\phi^b \quad (1)$$

where τ_f is the shear stress at failure state of unsaturated soil, c' is the effective cohesion intercept, ϕ' is the effective angle of internal friction of the saturated soil, ϕ^b is the angle of strength increase with respect to matric suction, $(\sigma_n - u_a)_f$ and $(u_a - u_w)_f$ are the net normal stress and the matric suction on the failure surface, respectively. When the specimen is saturated the pore-air pressure (u_a) will be replaced by pore-water pressure (u_w)

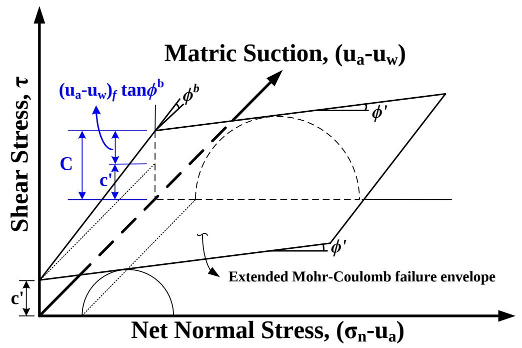

Fig. 7 Total cohesion under extended Mohr-Coulomb theory

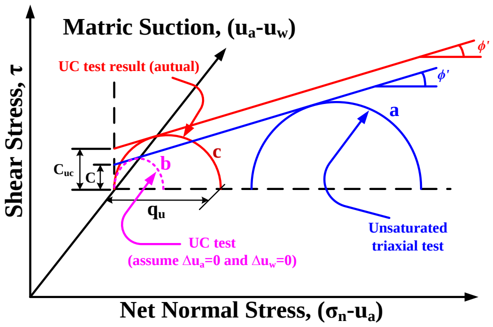

Fig. 8 Relationship between C and C_{uc}

and $(\sigma_n - u_a)_f$ can be converted to $(\sigma_n - u_w)_f$. Consequently, Eq. (1) could be rewritten as Eq. (2), which is the same as the Mohr-Coulomb failure criterion for saturated soils.

$$\tau_f = c' + (\sigma_n - u_w)_f\ tan\phi' \tag{2}$$

Ho and Fredlund (1982) proposed the concept of total cohesion under the framework of the three-dimensional extended Mohr-Coulomb Failure Criterion. The idea is to consider the contribution of the matric suction as an additional cohesion to facilitate its application for engineering practice. The effective cohesion is added to the matric suction term to get the total cohesion, C, as given in Eq. (3). Fig. 7 illustrates the physical meaning of the total cohesion, which is the intersection of the extended Mohr-Coulomb failure surface and the plane of zero net normal stress.

$$C = c' + (u_a - u_w)_f\ tan\phi^b \tag{3}$$

3.2 Relationship between unconfined compression test and total cohesion

The unconfined compression strength has been found to be positively related to the total cohesion obtained from the unsaturated triaxial test (Lin *et al.* 2016). However, the amount exhibits some difference. A regression approach has been adopted to quantify the relationship between the unconfined compression strength and the total cohesion using the experimental results, as to be discussed in the next section. As an attempt to provide a reasonable rationale for the regression Fig. 8 is a schematic attempting to qualitatively examine correlation of the unconfined compression test and the total cohesion based on the extended Mohr-Coulomb model. Because unsaturated soil has matric suction, the Mohr circle at failure of the triaxial test shall be on the $(u_a - u_w) \neq 0$ plane, shown in Fig. 8 as Mohr circle a. The total cohesion corresponding to the failure envelope is C value. For the same soil specimen (i.e., same soil fabric and engineering behavior), if the unsaturated unconfined compression test is conducted under the same matric suction, and if there is no change in pore-air pressure u_a or pore-water pressure u_w (i.e., assuming the pore air pressure and pore water pressure are not changed in the test process), the failure envelope shall be the same as the unsaturated triaxial test result. Therefore, the Mohr circle of the unsaturated unconfined compression test would be Mohr circle b in Fig. 8.

Although the changes in pore-water pressure u_w cannot be measured during the unsaturated unconfined compression test, the measurement of pore-water pressure u_w in the unsaturated triaxial test shows that the variation of u_w during the specimen loading is about 4-6 kPa, which is only about 1% of the deviator stress which is in the range of 400-600 kPa. Based on this observation, pore-water pressure is assumed unchanged during the unconfined compression test. However, the change in pore-air pressure u_a in the test process is expected to be more significant than pore water pressure change and its effect shall not be neglected. The Mohr circle size of the unsaturated unconfined compression test should be different from Mohr circle b. Thus, the actual unconfined compression test result may be Mohr circle c in Fig. 8.

According to the principle of effective stress, the effective friction angle ϕ' should be the same for the unconfined compression test and the triaxial test. Therefore, the total cohesion C_{uc} of the unsaturated unconfined compression test can be obtained, as shown in Mohr circle c of Fig. 8. It is expected that there shall exist a correlation function between the total cohesion C_{uc} obtained by the unsaturated unconfined compression test and the total cohesion C of the unsaturated triaxial test. The relationship can be expressed as Eq. (4), where α is defined as the proportion function. This proportion function α will be further examined in the subsequent sections. The C_{uc} value can be determined from the unsaturated unconfined compression strength q_u as Eq. (5). The unsaturated triaxial total cohesion C can be evaluated by Eq. (3), as suggested by Ho and Fredlund (1982). If the proportion function can be determined with sound rationale it may be possible to develop a simple alternative to estimate the total cohesion using the unconfined compression test.

$$\alpha\, C_{uc} = C \tag{4}$$

$$C_{uc} = \frac{q_u}{2} \times \frac{(1 - sin\phi')}{cos\phi'} \tag{5}$$

4. Experiment results

4.1 Unconfined compression test

Soil specimens compacted at three different initial

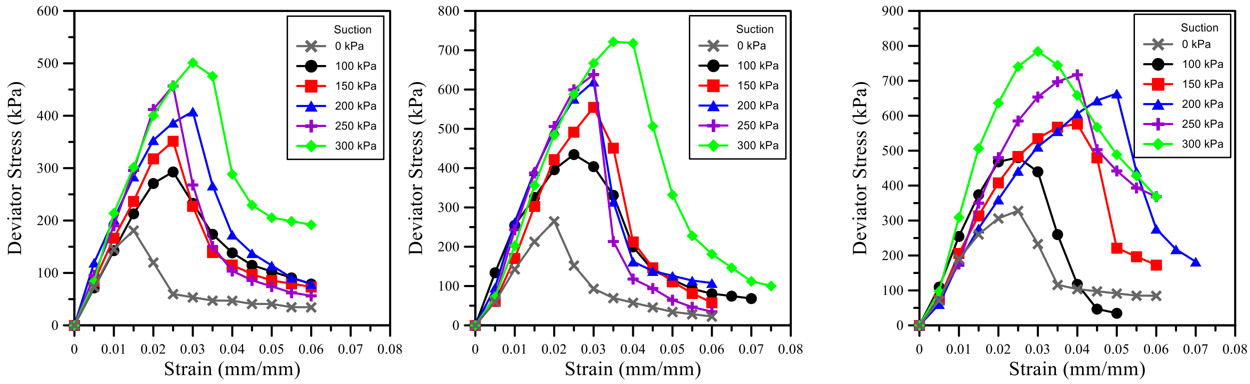

(a) OMC-3% (DRY) (b) OMC (c) OMC+3% (WET)

Fig. 9 Results of unconfined compression strength test

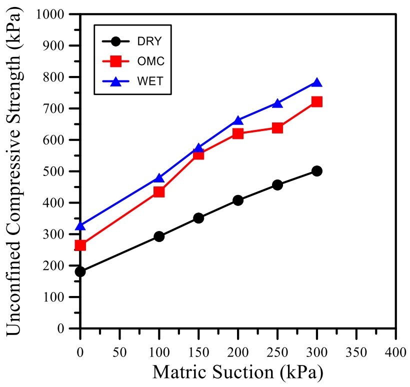

Fig. 10 Unconfined compression strength and matric suction

Table 1 Results of unconfined compression test

Compaction State	DRY		OMC		WET	
$u_a - u_w$ (kPa)	q_u(kPa)	C_{uc}(kPa)	q_u(kPa)	C_{uc}(kPa)	q_u(kPa)	C_{uc}(kPa)
0	181.06	53.10	264.99	67.35	328.08	89.62
100	292.93	86.41	434.87	110.53	480.32	131.21
150	351.52	103.70	554.91	141.04	576.45	157.47
200	408.00	120.36	620.24	157.64	663.58	181.27
250	456.97	134.80	638.45	162.27	717.62	196.04
300	501.26	147.87	721.82	183.46	784.53	214.31

Table 2 Total cohesion and ϕ^b value of unsaturated triaxial test

Compaction State	DRY		OMC		WET	
$u_a - u_w$ (kPa)	C(kPa)	ϕ^b(°)	C(kPa)	ϕ^b(°)	C(kPa)	ϕ^b(°)
0	23.49	28.92	39.47	36.11	48.96	32.70
100	68.77	24.36	85.27	24.77	101.19	27.58
200	100.44	17.57	116.05	17.00	132.11	17.18
300	124.87	13.73	135.71	11.13	149.82	10.04

Note: $\phi^b = \phi'$ and $C = c'$ when matric suction equals to zero

compaction conditions (OMC-3%, OMC, OMC+3%) are pretreated by the wetting and the drying apparatus to the target matric suction following the procedure described in Section 2.3. Then, the unconfined compression tests are conducted. The test results of three sets of samples of different initial compaction conditions are shown in Fig. 9. In addition to the matric suction of 100-300 kPa, the soil samples compacted at three different initial conditions and saturated by the wetting process are also included in Fig. 9 for the reference of zero matric suction. Test results show that the unconfined compressive strength increases significantly with matric suction regardless of the initial compaction condition, as expected. The stress-strain results of all the unsaturated soil specimens exhibit peak and post peak behavior.

The unconfined compressive strengths of three test sets are plotted together versus matric suction in Fig. 10. The effects of wetting and drying are similar regardless of the initial compaction condition. The unconfined compression strength is lowest when the sample is wetted to zero matric suction and increases when subjected to the subsequent drying due to matric suction increase. Interestingly, the unconfined compressive strength exhibits linear increasing relationship with matric suction within the range of 0 to 300 kPa. This phenomenon is consistent with the findings reported by Villar (2006). Villar (2006) concluded that the relationship of the unsaturated soil strength and the matric suction is approximately linear at low suction; however, when the matric suction is larger than a certain value the strength increase becomes mild. Therefore, the relationship shown in Fig. 10 may become nonlinear if the matric suction is higher than 300 kPa. This issue warrants further study.

Fig. 10 also shows the effects the initial compaction condition on the unsaturated shear strength. Under the same matric suction the strength of the DRY set is the lowest and the WET set is slightly larger than the OMC because the dry side sample adsorbed more water upon the wetting process to saturation as explained in Section 2.2 where SWCCs are presented. In general, the trend of the strength results is consistent with the results of the SWCCS. Therefore, the wetting and drying process does significantly influence the soil retention behavior and the unsaturated soil strength. Yang *et al.* (2004) have reported similar findings. Based on the unconfined compressive strength (q_u) in Fig. 10 the total cohesion C_{uc} of the unconfined compression test can be obtained using Eq. (5). The effective friction angles for

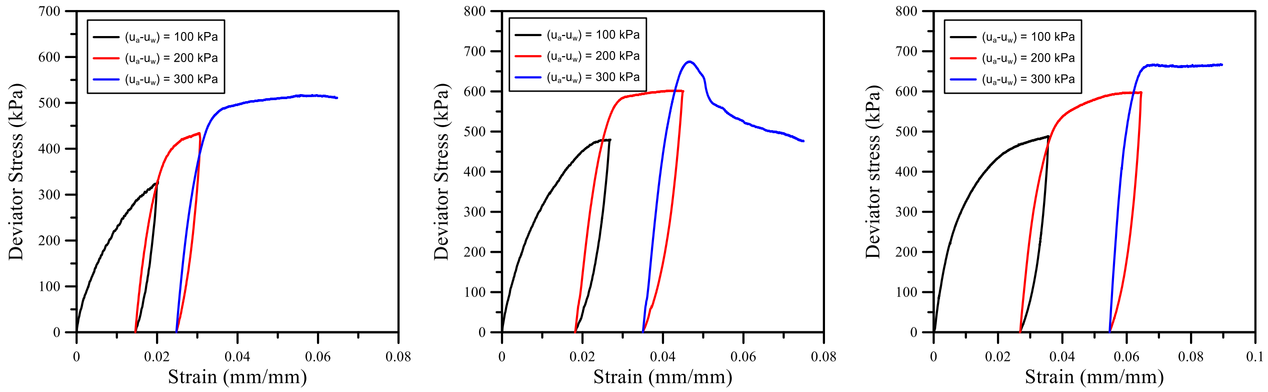

(a) OMC-3% (DRY) (b) OMC (c) OMC+3% (WET)

Fig. 11 Stress-strain curves of unsaturated triaxial test

Table 3 Parameter values of hyperbolic total cohesion model

Compaction state	c′(kPa)	a	b (1/kPa)	R^2
DRY	23.49	1.8809	0.003631	0.9998
OMC	39.47	1.7251	0.004628	0.9997
WET	48.96	1.3964	0.005243	0.9995

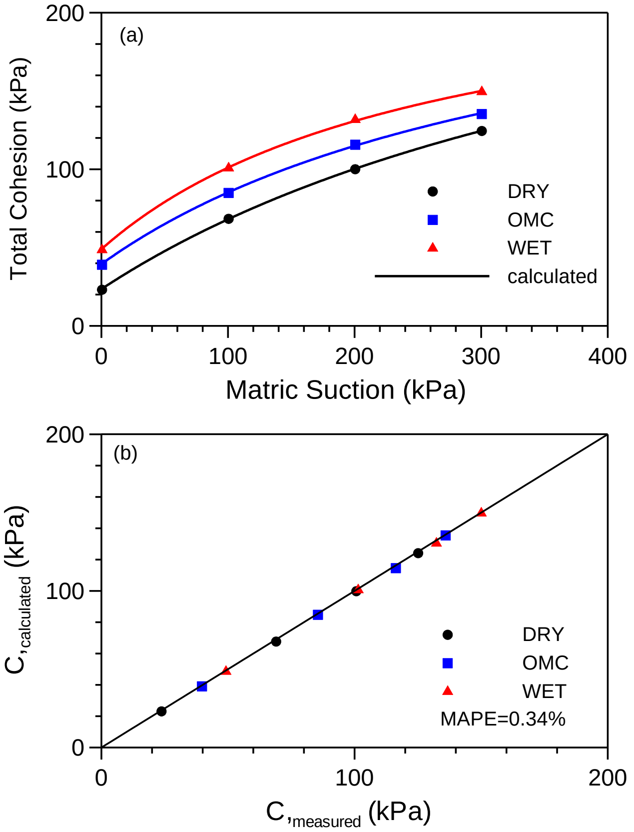

Fig. 12 Comparison of measured and calculated total cohesion: (a) Total cohesion vs. matric suction and (b) MAPE

DRY, OMC, and WET are 28.92, 36.11, and 32.70 degrees respectively. The calculated results are summarized in Table 1 for further study by comparing with the results of the unsaturated triaxial test.

4.2 Unsaturated triaxial test

The multistage unsaturated triaxial test is adopted in this study as has been described in Section 2.4. Three specimens of different initial compaction conditions are placed in the unsaturated triaxial cell. All of the samples are pre-saturated and the specified suction is applied and maintained until balance before the deviatoric loading. The deviator stress versus strain relationships are shown in Fig. 11. In general, test results are reasonable. The deviator stress increases with the matric suction for all three initial compaction conditions. In addition, the stress-strain trend and the deviator stress magnitude of the OMC and the WET are similar, as shown in Figs. 11(b) and 11(c). However, the DRY sample exhibited somewhat lower deviator stress under the same matric suction. This behavior is consistent with the results of the unconfined compression test and the rationale has been discussed in previous sections.

Using Eqs. (1) and (3), the total cohesion of unsaturated compacted lateritic soil specimens of different initial compaction condition and matric suction can be obtained. The ϕ^b value also can be calculated by the total cohesion equation of Eq. (3). The results are summarized in Table 2. The effective cohesion (c′) and the effective friction angle (ϕ′) corresponding to zero matric suction were determined from the saturated triaxial consolidated undrained test results. The test results reasonably reflect the influence of the as-compacted condition and also the effect of swelling during the saturation. They are denoted as *C* and ϕ^b at zero matric suction in Table 2. Regardless of the initial compaction state, the ϕ^b value decreases as the matric suction increases. This tendency and the range of the ϕ^b value are all in good agreement with previous findings reported in the literature (Fredlund and Rahardjo 1993). As a result, the total cohesion also exhibits a nonlinear increasing trend with the matric suction. It may be note that the specimen compacted at dry-of-optimum swelled the most significantly during the pre-saturation process and thus exhibits lower ϕ^b value than the wet side specimen. The effects of pre-saturation warrant further study.

Vilar (2006) and Lee *et al.* (2003) suggested that the nonlinear increase of total cohesion of unsaturated soil can be regressed by a hyperbolic function in terms of the matric suction, as Eq. (6) below.

$$C = c' + \frac{(u_a - u_w)}{a + b \times (u_a - u_w)} \tag{6}$$

where c' is the effective cohesion representing the total cohesion at zero suction, $(u_a - u_w)$ is the matric suction, a and b are the coefficients of the hyperbolic regression function.

The parameter values of a and b in the hyperbolic regression function are summarized in Table 3. Fig. 12 compares the total cohesion determined from the unsaturated triaxial tests and the values calculate using the hyperbolic function and the parameters given in Table 3. The calculated total cohesion values at different compaction state are in very good correlation with the test results as shown in Fig. 12(a). At present, this hyperbolic model is only validated with the test results of Linkuo lateritic soils. Whether it can be also applicable to other soils needs further study. The R^2 values are given in Table 3. In addition, the MAPE (mean absolute percentage error) of Eq. (7) can be used to determine the error between the calculated result and the measured value (Lewis, 1982). A MAPE value of less than 10% indicates an excellent agreement; a MAPE value of 10%-20% indicates a good agreement; a MAPE value of 20%-50% indicates a reasonable agreement; a MAPE value greater than 50% indicates a poor agreement. The MAPE value shown in Fig. 12(b) is only 0.34% and far below 10%, indicating an excellent agreement. In short, the above examination further confirms the reasonability of the unsaturated triaxial test results for the subsequent study.

$$MAPE = \frac{1}{k}\sum_{i=1}^{k}\left|\frac{y_i - \hat{y}_i}{y_i}\right| \tag{7}$$

where y_i= measured value, $\hat{y}_i$= model analysis value, and k= number of analytic data.

As a preliminary predictability check, an additional triaxial test of the OMC sample was conducted. The matric suction and the total cohesion are 400 kPa and 148.1 kPa, respectively. The total cohesion calculated by Equation (6) using the relevant parameters in Table 3 is 151.3 kPa. The predicted result agrees well with the test result. Further study with more extensive tests are warranted to confirm its predictability.

5. Total cohesion estimation using unconfined compression test

Based on the concept illustrated in Fig. 8, the relationship between the total cohesion (C) and the unconfined compressive strength (q_u) can be derived as Eq. (8) by substituting Eq. (5) into Eq. (4). Thus, the total cohesion could be evaluated from Eq. (8) based on the unconfined compression strength when the proportionality factor α is determined.

$$C = \alpha C_{uc} = \alpha \times \frac{q_u}{2} \times \frac{(1 - sin\phi')}{cos\phi'} \tag{8}$$

The definitions of the symbols of the above equation are the same as that of Eqs. (4) and (5).

Fig. 13 shows the relationship of the total cohesion (C)

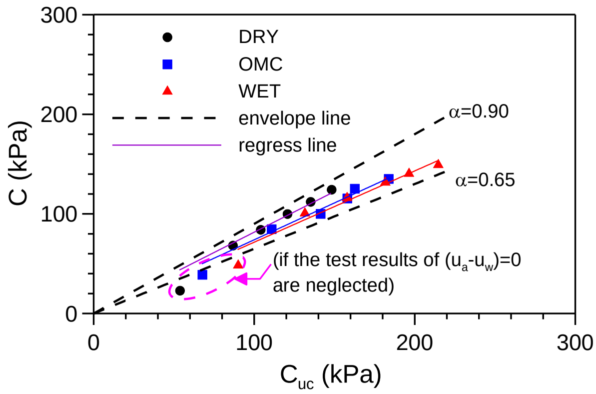

Fig. 13 Comparison of total cohesion of C and C_{uc}

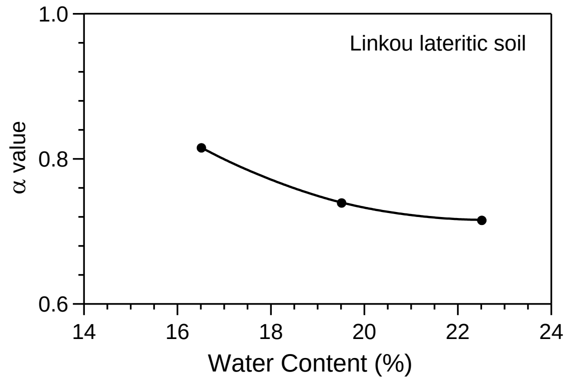

Fig. 14 Relationship between the α value and water content

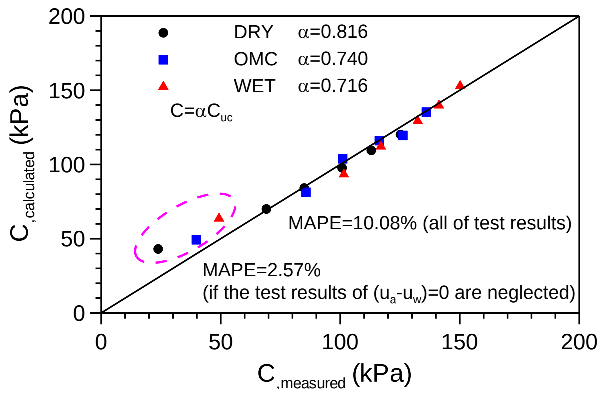

Fig. 15 Comparison of measured and calculated total cohesion by Eq. (8)

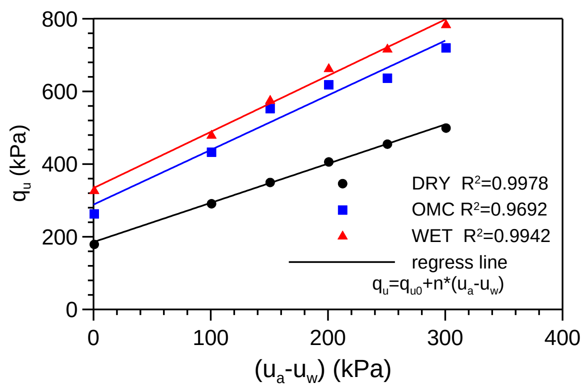

Fig. 16 Unconfined compression strength and matric suction

Table 4 Parameters for Eq. (10)

Compaction state	ϕ'(°)	α	q_{uo}(kPa)	n
DRY	28.92	0.816	185.43	1.079
OMC	36.11	0.740	288.59	1.504
WET	32.70	0.716	334.00	1.547

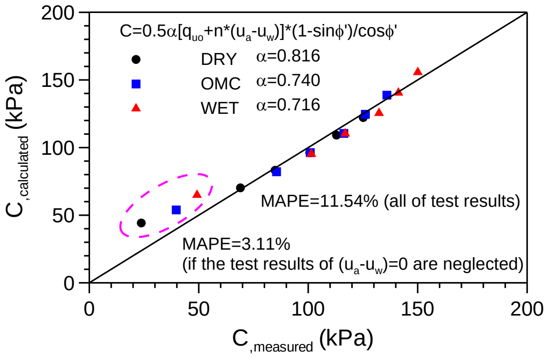

Fig. 17 Comparison of measured and calculated total cohesion by Eq. (10)

obtained from the unsaturated triaxial test results (Table 2) and the total cohesion (C_{uc}) derived from the unconfined compression results (Table 1). The results show that the unsaturated triaxial total cohesion C value is approximately in linear increasing relation to the total cohesion of the unconfined compression C_{uc} value. The proportionality constant α is in the range of about 0.65-0.90 for different compaction conditions, as shown in Fig. 13. This result represents the lower and upper limit of the proportion function for Linkou lateritic soil. Thus, the α value can be adopted to estimate the total cohesion from the unconfined compression test result when the soil initial condition is unknown. In specific, the α value is 0.816, 0.740 and 0.716 for the dry side, OMC and the wet side, respectively. These α values are all within the upper and lower bounds shown in Fig. 13. Furthermore, the α value exhibits a nonlinearly decreasing relation to the initial compacted water content, as shown in Fig. 14. Therefore, the α value can also be determined when the initial compacted water content is given.

Fig. 15 shows the comparison of the test results with the total cohesion values obtained by Eq. (8). The total cohesion values at different initial compaction conditions are all close to the test results, with a MAPE value of 10.08%. If the test results of suction at zero condition are neglected, the MAPE value will decrease to 2.57%. Because of the MAPE value is slightly higher than 10%, thus, the simplified method to evaluate the total cohesion of the unsaturated triaxial test based on the unconfined compression strength in this study can be ranked in the very good category.

In addition, the test results show that the unconfined compression strength is linearly increasing with soil suction, as shown in Fig. 16, and could be expressed as Eq. (9). As a result, the unconfined compression strength q_u could be estimated by the matric suction of the soil. Substituting Eq. (9) into Eq. (8), the total cohesion prediction equation could be written as Eq. (10). Therefore, the total cohesion of the unsaturated triaxial test could be directly evaluated by the unconfined compression strength of the unsaturated soil when the parameters, α, q_{u0} and n are determined. The parametric values of Eq. (10) are summarized in Table 4.

Fig. 17 illustrates the comparison of the test results with the total cohesion values calculated by Eq. (10). The total cohesion values at different initial compaction states are also close to the test results, with a MAPE value of 11.54%. When the test results of zero suction are excluded, the MAPE value decreased to 3.11%. Similarly, the MAPE value is also slightly higher than 10%. Thus, the total cohesion of the unsaturated soil can be estimated by the proposed simplified method using the unconfined compression strength. Both Eqs (8) and (10) can give reasonable results with about the same accuracy.

$$q_u = q_{u0} + n \times (u_a - u_w) \tag{9}$$

where q_{u0} and n are the intercept and the slope of the linear relationship between the unconfined compression strength and the matric suction of the soil, respectively. The parameter q_{u0} also represents q_u value at zero soil suction.

$$C = \frac{\alpha}{2} \times [q_{u0} + n \times (u_a - u_w)] \times \frac{(1 - sin\phi')}{cos\phi'} \tag{10}$$

6. Conclusions

1. A simplified method to estimate the total cohesion of the Linkuo lateritic unsaturated soil by using an unconfined compression test is proposed in this study. The results are promising and show good potential for practical application. However, the matric suction studied was below 300 kPa and only limited values of the matric suction were examined. The proposed method is potentially applicable to geotechnical problems such as the stability analysis of the unsaturated soil slope subjected to rainfall infiltration. However, further study is warranted for validation.

2. The total cohesion (C_{uc}) of the unsaturated lateritic soil estimated by the unconfined compression test exhibits a strong positive relationship with the unsaturated triaxial total cohesion (C). The matric suction has been shown to act as a key parameter to bridge these two total cohesions. Based on the unsaturated triaxial test results of matric suction below 300 kPa, the proportion ratio of C to C_{uc} ranges from 0.65 to 0.90.

3. When the proportionality constant α is determined by the unconfined compression test results and used to evaluate the total cohesion the unsaturated triaxial test, the MAPE value is about 10.08-11.54% which is only slightly higher than 10%. Consequently, the simplified method derived in this study based on the unconfined compression test exhibits good predictive ability.

4. The unconfined compressive strength increases significantly with the matric suction for all specimens initially compacted at OMC-3%(DRY), OMC, and OMC+3%(WET). The trend is the same for three different initial compaction conditions. However, the magnitude exhibits a more complicated behavior. In general, the

compressive strength of the OMC and the WET specmens are close to each other. However, the value of the DRY specimen is the lowest mainly due to larger swelling during the saturation process before applying the target matric suction.

5. Results of the unsaturated triaxial tests show a clear trend of strength increase with matric suction despite its initial compaction condition. The effects of the initial compaction condition on the strength are similar to the unconfined compressive test. The unsaturated triaxial test result also shows that the ϕ^b value decreases as the matric suction increases. In addition, the total cohesion exhibits a hyperbolic relationship with the matric suction. These behaviors are in good agreement with previous findings reported

Acknowledgements

This study was financially supported by the Ministry of Science and Technology of Taiwan. This support is gratefully acknowledged. The authors would also like to thank technical staff H. Y. Chen of National Taiwan University of Science and Technology for his assistance in laboratory testing and graduate students J. H. Li and K. E. Ting for their assistance in preparing this paper.

References

Cho, G.C. (2016), "Geotechnical engineering for sustainable development", *Proceedings of the 2016 World Congress on Advances in Civil, Environmental and Materials Research (ACEM16)*, Jeju, Korea, August.

Estabragh, A.R. and Javadi, A.A. (2012), "Effect of suction on volume change and shear behaviour of an overconsolidated unsaturated silty soil", *Geomech. Eng.*, **4**(1), 55-65.

Fredlund, D.G. and Morgenstern, N.R. (1977), "Stress state variables for unsaturated soils", *J. Geo. Eng.*, **103**(5), 447-466.

Fredlund, D.G., Morgenstern, N.R. and Wider, R.A. (1978), "The shear strength of unsaturated soils", *Can. Geotech. J.*, **15**(3), 313-321.

Fredlund, D.G. and Rahardjo, H. (1993), *Soil Mechanics for Unsaturated Soils*, John Wiley & Sons, New York, U.S.A.

Ho, D.G. and Fredlund, D.G. (1982), "A multistage triaxial test for unsaturated soils", *Geotech. Test. J.*, **5**(1), 18-28.

Jiang, Y.S. (2014), "Characteristics of total cohesion and shear strength of unsaturated compacted lateritic soils", M.Sc. Thesis, National Taiwan University of Science and Technology, Taipei, Taiwan.

Kim, Y., Park, H. and Jeong, S. (2017), "Settlement behavior of shallow foundations in unsaturated soils under rainfall", *Sustainability*, **9**(8), 1-13.

Lewis, C.D. (1982), *Industrial and Business Forecasting Method*, Butterworth Scientific Publishers, London, U.K.

Lee, S.J., Lee, S.R. and Kim, Y.S. (2003), "An approach to estimate unsaturated shear strength using neural network and hyperbolic formulation", *Comput. Geotech.*, **30**(6), 489-503.

Lin, H.D., Kung, J.H.S., Wang, C.C., Liao, C.Y. and Tsai. M.F. (2010), "Stability analysis of unsaturated soil slope subjected to rainfall infiltration", *Proceedings of the 4th Japan-Taiwan Joint Workshop on Geotechnical Hazards from Large Earthquakes and Heavy Rainfalls*, Sendai, Japan, October.

Lin, H.D., Wang, C.C. and Kung, J.H.S. (2015), "Wetting and drying on matric suction of compacted cohesive soil", *Proceedings of the ISOPE-2015, the 25th International Ocean and Polar Engineering Conference*, Kona, Big Island, Hawaii, U.S.A., June.

Lin, H.D., Jiang, Y.S., Wang, C.C. and Chen, H.Y. (2016), "Assessment of apparent cohesion of unsaturated lateritic soil using an unconfined compression test", *Proceedings of the 2016 World Congress on Advances in Civil, Environmental and Materials Research (ACEM16)*, Jeju, Korea, August.

Lin, H.D., Wang, C.C. and Jhou, B.H. (2017), "A study of the apparent cohesion and shear strength characteristics of unsaturated compacted lateritic soil", *J. Technol.*, **32**(3), 117-185.

Ng, C.W.W., Sadeghi, H., Hossen, B., Chiu, C.F., Alonso, E.E. and Baghbanrezvan, S. (2016), "Water retention and volumetric characteristics of intact and re-compacted loess", *Can. Geotech. J.*, **53**(8), 1258-1269.

Nyunt, T.T., Leong, E.C. and Rahardjo, H. (2011), "Stress-strain behavior and shear strength of unsaturated residual soil from triaxial tests", *Proceedings of the 5th Asia-Pacific Conference on Unsaturated Soils: Theory and Practice*, Pattaya, Thailand, November.

Oh, W.T and Vanapalli, S.K. (2011), "Modelling the applied vertical stress and settlement relationship of shallow foundations in saturated and unsaturated sands", *Can. Geotech. J.*, **48**(3), 425-438.

Rahardjo, H., Meilani, I. and Leong, E.C. (2009), "Shear strength characteristics of a compacted soil under infiltration conditions", *Geomech. Eng.*, **1**(1), 35-52.

Shou, K.J., Wu, C.C. and Lin, J.F. (2018), "Predictive analysis of landslide susceptibility under climate change conditions-a study on the Ai-Liao watershed in southern Taiwan", *J. GeoEng.*, **13**(1), 13-27.

Tekinsoy, M.A., Kayadelen, C., Keskin, M.S. and Soylemez, M. (2004), "An equation for predicting shear strength envelope with respect to matric suction", *Comput. Geotech.*, **31**(7), 589-593.

Tang, Y., Taiebat, H.A. and Senetakis, K. (2017), "Effective stress based bearing capacity equations for shallow foundations on unsaturated soils", *J. GeoEng.*, **12**(2), 59-64.

Vanapalli, S.K., Fredlund, D.G., Pufahl, D.E. and Clifton, A.W. (1996), "Model for the prediction of shear strength with respect to soil suction", *Can. Geotech. J.*, **33**(3), 379-392.

Vilar, O.M. (2006), "A simplified procedure to estimate the shear strength envelope of unsaturated soils", *Can. Geotech. J.*, **43**(10), 1088-1095.

Wang, C.C., Kung, J.H. S., Liao, C.Y. and Lin, H.D. (2010), "Experimental study on matric suction of unsaturated soil upon drying and wetting", *Proceedings of the 3rd International Conference on Problematic Soils*, Adelaide, Australia, April.

Yang, H., Rahardjo, H., Leong, E.C. and Fredlund, D.G. (2004a), "Factors affecting drying and wetting soil-water characteristic curves of sandy soils", *Can. Geotech. J.*, **41**(5), 908-920.

Yang, S.R., Lin, H.D., Kung, H.S.J. and Liao, J.Y. (2008), "Shear wave velocity and suction of unsaturated soil using bender element and filter paper method", *J. GeoEng.*, **3**(2), 67-74.

Yang, S.R., Lin, H.D., Kung, H.S.J. and Huang, W.C. (2008), "Suction-controlled laboratory test on resilient modulus of unsaturated compacted subgrade soils", *J. Geotech. Geoenviron. Eng.*, **134**(9), 1375-1384.

Yang, S.R., Lin, H.D. and Huang, W.H. (2012), "Variation of initial soil suction with compaction conditions for clayey soils", *J. Mech.*, **28**(3), 431-437.

Zhang, L.L., Fredlund, D.G., Fredlund, M.D. and Wilson, G.W. (2014), "Modeling the unsaturated soil zone in slope stability analysis", *Can. Geotech. J.*, **51**(12), 1384-1398.

GC